

1 Comparing submarine and fluvial channel kinematics:  
2 Implications for stratigraphic architecture

3 **Zane R. Jobe<sup>1\*</sup>, Nick C. Howes<sup>1</sup>, and Neal C. Auchter<sup>2</sup>**

4 *<sup>1</sup>Shell International Exploration and Production Inc., Houston, Texas 77079, USA*

5 *<sup>2</sup>Department of Geosciences, Virginia Polytechnic Institute, Blacksburg, Virginia 24060,*  
6 *USA*

7 \*Current Address: Colorado School of Mines, Golden, Colorado 80401, USA; E-mail:  
8 zanejobe@mines.edu.

9 **ABSTRACT**

10 Submarine and fluvial channels exhibit qualitatively similar geomorphic patterns,  
11 yet produce very different stratigraphic records. We reconcile these seemingly  
12 contradictory observations by focusing on the channel-belt scale and quantifying the  
13 time-integrated stratigraphic record of the belt as a function of (1) the geometric scale and  
14 (2) the trajectory of the geomorphic channel, applying the concept of stratigraphic  
15 mobility. By comparing 297 submarine and fluvial channel belts from a range of tectonic  
16 settings and time intervals, we identify channel kinematics (trajectory) rather than  
17 channel morphology (scale) as the first order control on stratigraphic architecture and  
18 show that seemingly similar channel forms (in terms of scaling) have the potential to  
19 produce markedly different stratigraphy. Submarine channel-belt architecture is  
20 dominated by vertical accretion (aggradational channel fill deposits), in contrast to fluvial  
21 systems that are dominated by lateral accretion (point bar deposits). This difference is  
22 best described with the channel-belt aspect ratio, which is 9 for submarine systems and

23 72 for fluvial systems. Differences in channel kinematics and thus stratigraphic  
24 architecture between the two environments appear to result from markedly different  
25 coupling between channel aggradation and overbank deposition. The methodology and  
26 results presented here are also applicable to interpreting channelized stratigraphy on other  
27 planets and moons.

## 28 **INTRODUCTION**

29 Sinuous submarine and fluvial channels have qualitatively similar planform  
30 morphologies, but very different preserved stratigraphic records (Flood and Damuth,  
31 1987; Kolla et al., 2007). Sinuous fluvial channel belts are dominated by lateral migration  
32 deposits, including point bars and oxbow cutoffs (Allen, 1965; Sun et al., 1996) and  
33 undergo only minor aggradation ( $>1$  channel depth of super-elevation) prior to avulsion  
34 (Mohrig et al., 2000). Submarine channels, while displaying lateral migration (Abreu et  
35 al., 2003; Kolla et al., 2012), tend to have a more significant component of vertical  
36 aggradation (Peakall et al., 2000; Deptuck et al., 2007; Sylvester et al., 2011). Submarine  
37 channel-belt deposits are commonly offset to vertically stacked, sand-rich channel fill  
38 deposits (Macauley and Hubbard, 2013). This study quantifies the similarities and  
39 differences between submarine and fluvial channel belts and explores the formative  
40 processes that result in vastly different kinematics and stratigraphic architecture.

## 41 **CHANNEL KINEMATICS: TRAJECTORY AND MOBILITY**

### 42 **Definitions and Methodology**

43 Jerolmack and Mohrig (2007) introduced the channel mobility number (Equation  
44 1) as a metric to characterize and understand channel deposits. The mobility number is  
45 defined as the ratio of avulsion and lateral migration time scales. In a more general sense,

46 channel mobility describes a channel trajectory scaled by the dimensions of the  
47 geomorphic channel form. For applications to modern rivers, channel trajectory can be  
48 expressed as the ratio of temporal rates of lateral ( $V_c$ ) and vertical ( $V_a$ ) migration  
49 (Jerolmack and Mohrig, 2007). Because we are interested in characterizing the preserved  
50 stratigraphic record of channel trajectory where rate data (i.e.,  $V_a$ ,  $V_c$ ) are uncommon, we  
51 propose a stratigraphic mobility number,  $M_s$ .

52 We recast the mobility equation, by substituting the temporal rates ( $V_c/V_a$ ) with  
53 the relative spatial displacements ( $L_c/L_a$ ) of the channel as measured in a strike-oriented  
54 cross section (Fig. 1; Equation 2). The two formulations ( $M$  and  $M_s$ ) are conceptually  
55 identical if considered over the same time-period. The ‘local’ stratigraphic trajectory  
56 ( $L_c/L_a$ ) can be thought of as spatially separated points that denote the spatial path of the  
57 channel thalweg/centerline through time, where each point along the path represents an  
58 easily identifiable location of the channel thalweg (Fig. 1C; cf. ‘discrete migration  
59 events’ of Deptuck et al., 2007; Kolla et al., 2007). We also define an aggregate or belt  
60 averaged stratigraphic mobility number,  $M_{sb}$ , using the channel belt dimensions  
61 (Equation 3). Channel belt width ( $B_{cb}$ ) and thickness ( $H_{cb}$ ) are defined as the maximum  
62 lateral and vertical extent of the belt (including the youngest channel form), respectively  
63 (Fig. 1). Channel width ( $B$ ) and thickness ( $H$ ) were estimated from the final channel form  
64 (Fig. 1). Note that  $B_{cb}$  and  $H_{cb}$  are minimum estimates because we do not include any  
65 coeval overbank or levee deposits.

66 
$$M = \frac{V_c \bar{h}}{V_a B}, \quad (1)$$

67 
$$M_{sl} = \frac{L_c H}{L_a B}, \quad (2)$$

68 
$$M_{sb} = \frac{(B_{cb}-B) H}{(H_{cb}-H) B} . \quad (3)$$

69 The local ( $M_{sl}$ ) and belt-averaged ( $M_{sb}$ ) methods calculate the stratigraphic  
70 mobility number at the scale of individual channel migration events and the entire  
71 channel belt scale, respectively (Fig. 1). While the stratigraphic record is biased toward  
72 the preservation of net-aggradational channel belts that produce  $M_s > 0$ , negative values  
73 of  $M_s$  describe degradational phases of channel belt evolution or net-degradational fluvial  
74 and submarine channel belt deposits. Because  $M_{sl}$  is calculated using each  $L_c/L_a$  point  
75 pair of the channel trajectory, it has a broader distribution of values than  $M_{sb}$ . In both  
76 definitions, large values of  $M_s$  result from channels with abundant lateral migration but  
77 little aggradation relative to the size of the geomorphic channel form.

## 78 **Data Sources and Interpretation**

79 This study compiles 297 channel trajectory and channel-form geometry  
80 measurements from a global sampling of 21 submarine systems and 13 fluvial systems  
81 (Fig. 1B; Table DR1 in the GSA Data Repository<sup>1</sup>). Data sources include seismic-  
82 reflection cross-sections and outcrop exposures. In order to standardize measurements,  
83 we utilized a simple set of guidelines based on observable seismic/outcrop facies and  
84 geometries (Fig. 1C; see the Data Repository). We define a channel belt as a coherent  
85 package of channel-related deposits that does not contain significant erosion (i.e.,  $>1$   
86 channel depth). Thus, channel belts are separated by avulsion or significant erosion  
87 events that reset the geomorphic channel surface. This definition of channel belt does not  
88 imply an absolute temporal duration, only the relative time of channel belt formation,  
89 which may vary by system.

90 Trajectory data ( $L_c$ ,  $L_a$ ) were collected for each channel belt at the basal  
91 terminations of inclined reflectors/surfaces from selected cross sections, with the  
92 assumption that these points closely approximate the coeval channel thalweg (Fig. 1).  
93 The spacing of recorded trajectory points was dictated by observable reflectors/surfaces  
94 (Fig. 1C). Channel forms were interpreted based on concave up geometries, internal lap-  
95 out geometries, and vertical transition to horizontal, parallel, laterally continuous  
96 reflectors (Fig. 1C). Some channel forms were truncated by subsequent erosion and thus  
97 form minimum values of  $B$  and  $H$ . We acknowledge that the measurement of channel  
98 form within the stratigraphic record can be difficult and at times may differ from the  
99 geomorphic channel form. However, our measurements of  $B$ ,  $H$ , and  $B/H$  (aspect ratio)  
100 generally agree with measurements from modern topographic and bathymetric data (Fig.  
101 DR1), indicating that better preservation and/or decompaction of the channel form would  
102 not significantly alter the results of this study. Interestingly, the  $B/H$  data from Jerolmack  
103 and Mohrig (2007) is quite different from all other sources, likely due to their focus on  
104 anastomosing and distributary systems (see the Data Repository; Fig. DR1).

## 105 **COMPARISONS OF SUBMARINE AND FLUVIAL DATA**

### 106 **Channel and Channel Belt Dimensions**

107 Channel and channel-belt width ( $B$ ,  $B_{cb}$ ) are broadly similar for submarine  
108 channels and rivers, with submarine channels tending to be somewhat wider than rivers  
109 (Fig. 2; Fig. DR1). However, submarine channel and channel-belt thickness ( $H$ ,  $H_{cb}$ ) are  
110 4–5× thicker than their fluvial counterparts (Fig. 2). While the absolute dimensions (Figs.  
111 2A–D) display differences in width and thickness, normalized dimensions (Figs. 2E–G)  
112 are more useful to evaluate differences in lateral and vertical channel migration at the

113 channel-belt scale. Our data indicates that the median value of normalized channel belt  
114 width ( $B_{cb}/B$ ) for fluvial systems is 4.7, much greater than 2.1 for submarine systems  
115 (Fig. 2E). Normalized channel belt thickness ( $H_{cb}/H$ ) values have the opposite  
116 relationship, with median values for submarine systems (2.9) being almost twice that of  
117 fluvial systems (1.6; Fig. 2F). These results are summarized with the channel belt aspect  
118 ratio ( $B_{cb}/H_{cb}$ ) that describes the shape of the channel belt (Fig. 2G). Due to high  
119 aggradation (i.e., low values of  $L_c/L_a$ ), submarine channel belts tend to be thick and  
120 narrow, with a median value of  $B_{cb}/H_{cb} = 9$ , whereas fluvial channel belts are thin and  
121 wide, with a median value of 72 (Fig. 2G).

### 122 **Channel Kinematics: Trajectory and Stratigraphic Mobility**

123 Trajectory describes the shape of the path of a channel as it migrates in time and  
124 space to form a channel belt. A plot of  $L_c$  versus  $L_a$  presents the shape of the trajectories  
125 collected from seismic and outcrop channel belts (Fig. 3A). Fluvial and submarine  
126 trajectories have broadly similar ranges of  $L_c$  but submarine channels have  $\sim 10\times$  larger  
127 values of  $L_a$  (Fig. 3). Submarine channel trajectories clearly demonstrate a two-phase  
128 evolution that results in a hockey-stick trajectory shape: (1) a phase of lateral migration  
129 (sometimes with degradation), followed by (2) a phase of increasing  $L_a$  (i.e., increasing  
130 aggradation).

131 When calculating  $M_{sl}$ , the height above the base of the channel belt ( $z$  in Fig. 1A)  
132 can be normalized to  $H$ , allowing us to plot  $M_{sl}$  against the number of ‘aggraded channel  
133 depths’ (Fig. 3B). A temporal trend of lateral migration ( $M_{sl} \gg 0$ ) followed by increasing  
134 vertical aggradation ( $M_{sl} \geq 0$ ) is very robust for submarine channel belts (Fig. 3B).

135 Interestingly, the same trend is present for fluvial channel belts, albeit with 10× lower  
136 values of aggraded channel depths.

137 At the belt scale, submarine systems have much smaller values of  $M_{sb}$  than fluvial  
138 systems (Fig. 3C), with median values of 0.6 and 5.5, respectively. This order-of-  
139 magnitude difference indicates that during channel belt formation, submarine channels  
140 aggrade ~10x more than fluvial channels, resulting in a thicker, narrower channel belt  
141 (Fig. 2G) and thus lower  $M_{sb}$  values (Fig. 3C). If a submarine channel belt is evolving  
142 within larger-scale (i.e., canyon) confinement, this trend would be further exaggerated.

### 143 **CONTROLS ON CHANNEL KINEMATICS**

#### 144 **Why Do Submarine Channels Evolve from Lateral Migration to Aggradation?**

145 The hockey-stick shape of channel trajectory (i.e., decreasing  $M_{sl}$  through time in  
146 Fig. 3B) is consistent with conceptual models of submarine channel evolution (e.g.,  
147 Peakall et al., 2000; Deptuck et al., 2007; McHargue et al., 2011). However, this study is  
148 the first to quantify the trend with a global data set. Various mechanisms have been  
149 proposed to explain this evolution, including turbidity current flow properties (Kolla et  
150 al., 2007), progressive levee growth (Peakall et al., 2000), sediment supply versus  
151 accommodation (Kneller, 2003), and changes in equilibrium profile (Hodgson et al.,  
152 2011). Many studies invoke complex interactions between the above mechanisms. While  
153 we cannot exclude allogenic mechanisms, our data were collected over a range of  
154 tectonic settings, geologic-time intervals, and sediment supply regimes. Thus, we limit  
155 the present discussion to autogenic variables that must be present in every submarine  
156 channel system, regardless of tectonic setting or other allogenic controls.

157 We interpret that the flow properties unique to submarine channels are  
158 responsible for enhanced levee growth and the resultant aggradation. Flows in submarine  
159 channels have  $\sim 50\times$  less density contrast between flow and ambient fluid than rivers  
160 (Imran et al., 1999), enhancing super-elevation of the flow around bends. This increases  
161 the potential for overspill and flow stripping, which result in overbank deposition and  
162 levee growth (Piper and Normark, 1983; Straub et al., 2008). In addition, the velocity  
163 maximum in the vertical profile of a characteristic submarine flow is located much closer  
164 to the bed relative to its fluvial counterpart (Sequeiros et al., 2010), such that overbanking  
165 has a lower potential shear stress. Combined, these factors promote levee growth and  
166 discourage avulsion.

167 For a submarine channel to maintain a constant cross-sectional area locally, there  
168 must be coupling such that the thalweg aggrades as the levees grow or vice versa (e.g.,  
169 Imran et al., 1999). If either levee deposition (or thalweg deposition) occurs in isolation,  
170 the cross sectional area of the channel is perturbed, causing either flow expansion (or  
171 acceleration) (Exner equation, see Paola and Voller, 2005). This results in local  
172 deposition (or erosion) in the channel thalweg to return the cross sectional area to its  
173 original, equilibrium state. This depositional feedback results in aggradation of the entire  
174 channel belt. These processes are reflected in the high aggradational potential of  
175 submarine systems, which results in systematically thicker channel belts compared to  
176 fluvial systems and is reflected in larger values of  $H_{cb}/H$  (Fig. 2F). Dorrell et al. (2015)  
177 suggest that aggradational submarine channels are inherently unstable; we do not  
178 disagree, but argue that instability is a relative term and that submarine channels are  
179 much more stable under aggradational conditions than fluvial channels.



## 180 **Resultant Stratigraphic Architecture**

181 Normalized channel belt dimensions allow us to plot channel belts of differing  
182 scale to assess their ‘shape’ and spatiotemporal evolution (Fig. 4A). The threshold  
183 separating the dominance of lateral accretion versus ‘vertical accretion’ (i.e., aggradation)  
184 can be described by the equation

$$185 \quad \frac{B_{cb}}{H_{cb}} = \frac{B}{H}. \quad (4)$$

186 In cases where  $B_{cb}/H_{cb} \ll B/H$ , vertical accretion is the dominant form of  
187 stratigraphic preservation, and where  $B_{cb}/H_{cb} \gg B/H$ , lateral accretion is dominant.  
188 Equation 4 is plotted as a line in Figure 4A. All fluvial systems plot below the threshold  
189 line (Fig. 4A), indicating that lateral accretion is the dominant kinematic form. 73% of  
190 submarine systems plot above the threshold, indicating that vertical accretion (i.e.,  
191 aggradation) is dominant for the majority of submarine channel belts.

192 A schematic of the key differences in the evolution and channel belt dimensions  
193 of submarine and fluvial systems is presented in Figure 4B. Values of  $B_{cb}/B$  are variable  
194 for both submarine and fluvial systems, likely because  $B_{cb}/B$  is proportional to the belt  
195 maturity and floodplain erodability (cf. Sun et al., 1996). However, values of  $H_{cb}/H$  for  
196 submarine systems are commonly 2× and sometimes 10× larger than fluvial systems. The  
197 low stratigraphic mobility ( $M_s$ ) and high aggradational potential of submarine channel  
198 belts promotes the preservation of sandy channel fills and muddy levee and overbank  
199 deposits (e.g., Jobe et al., 2015), while high  $M_s$  and low aggradational potential of fluvial  
200 channel belts results in the preservation of sandy point bars and muddy oxbow deposits  
201 (Fig. 1).

## 202 **CONCLUSIONS**

203 Fluvial and submarine channels have qualitatively similar planform patterns, but  
204 very different stratigraphic records. Fluvial channel belts are relatively thin and  
205 dominated by lateral migration deposits, while submarine channel belts are very thick and  
206 contain more vertical accretion (i.e., aggradational channel-fill) deposits. Using a global  
207 data set, this study describes the dimensions, kinematics, and stratigraphic mobility of  
208 submarine and fluvial channel belts. Both submarine and fluvial systems exhibit a two-  
209 phase evolution of the channel trajectory, a phase of lateral migration (sometimes with  
210 degradation) and a phase of increasing aggradation while lateral migration decreases.  
211 However, submarine channel belts are 2× thicker and have 10× smaller stratigraphic  
212 mobility numbers than their fluvial counterparts. The channel belt aspect ratio best  
213 describes this relationship, with median values for submarine and fluvial systems of 9 and  
214 72, respectively. These results can be used to help interpret channelized stratigraphy on  
215 other planets and moons, where the distinction between fluvial and submarine deposition  
216 is often difficult. These data are collected from a range of tectonic settings and time  
217 intervals, suggesting that differences in channel kinematics and thus stratigraphic  
218 architecture in submarine channel systems are caused by flow properties of turbidity  
219 currents. We interpret that higher quantities of suspended sediment in upper portions of  
220 the flow and the position of the velocity maximum close to the bed cause enhanced levee  
221 development and thus aggradation of the channel belt.

## 222 **ACKNOWLEDGMENTS**

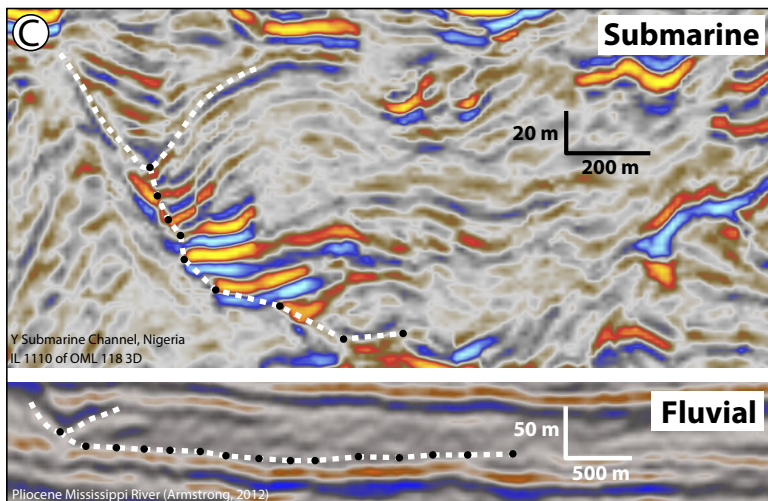
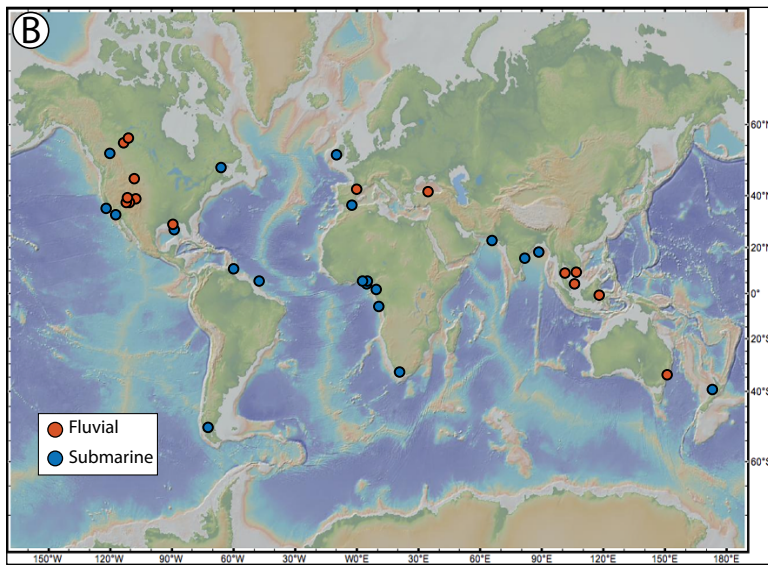
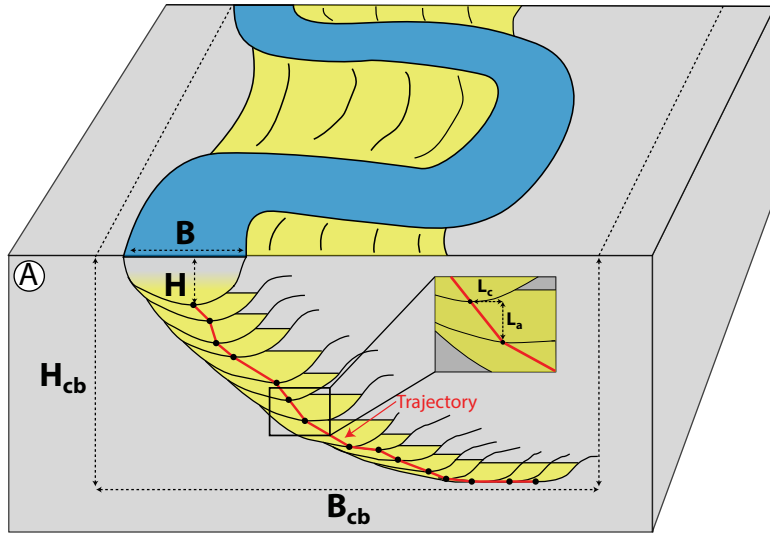
223 The authors would like to thank Shell International Exploration and Production  
224 for permission to publish. David Mohrig, Kyle Straub, and Tim Demko provided

225 insightful reviews that greatly improved the paper. Finally, this paper benefitted from  
226 discussions with Jake Covault, Steve Hubbard, and Brian Romans.

227

228

229 Figure 1. Kinematics of submarine and fluvial channels. A: Channel belt schematic.  
230 Local stratigraphic mobility  $M_{sl}$  is calculated using relative spatial displacements ( $L_c/L_a$ ),  
231 while belt-averaged  $M_s$  ( $M_{sb}$ ) is calculated using channel belt width and thickness aspect  
232 ratio  $B_{cb}/H_{cb}$ . B: Map of the data set utilized in this study, including 21 submarine and 13  
233 fluvial systems. C: Typical submarine and fluvial channel belts with interpretation  
234 overlain. Submarine channels are more aggradational and thus have lower  $M_s$  values.  
235



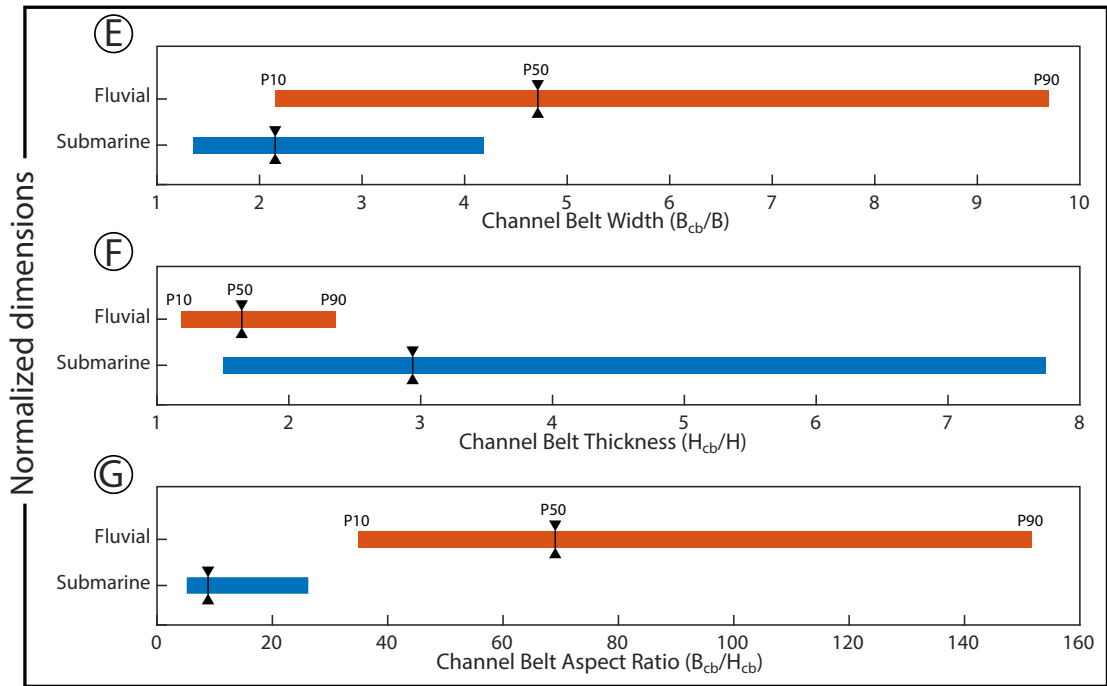
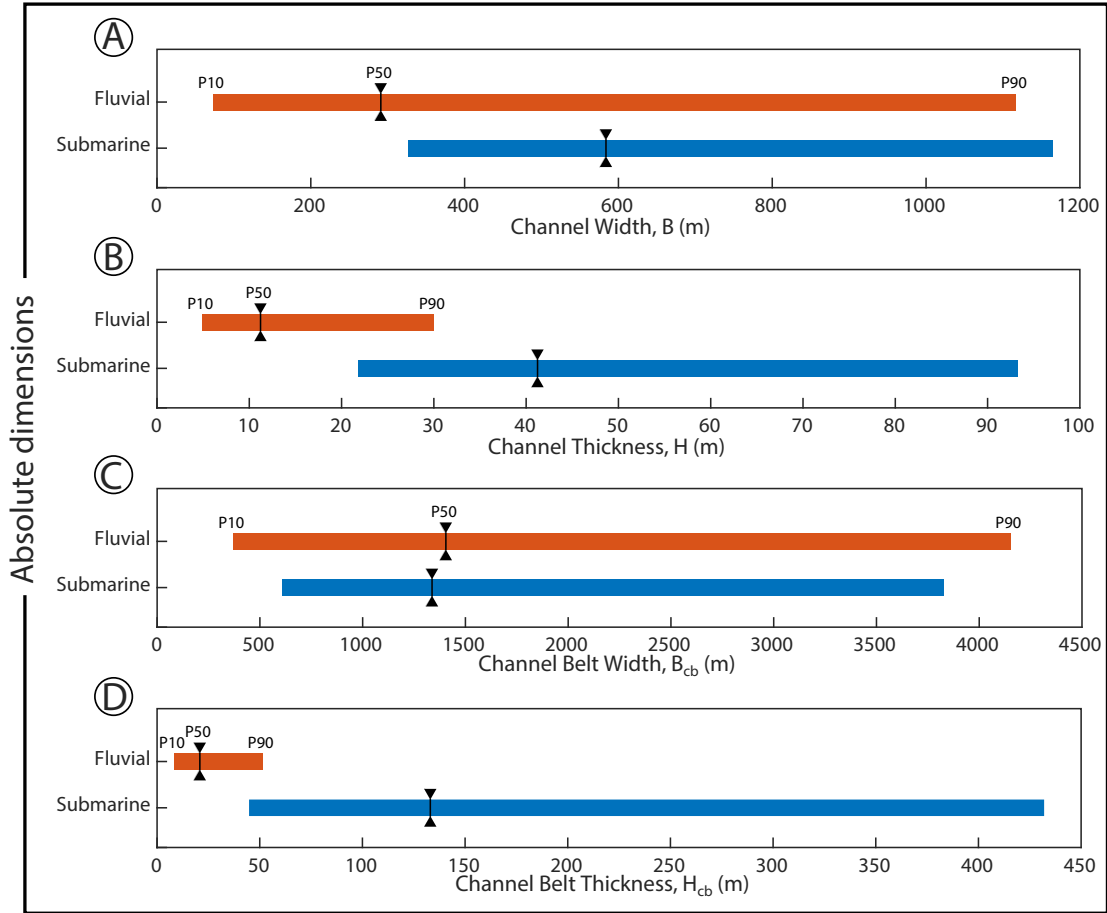
236

237 Figure 2. Absolute (A–D) and normalized (E–G) channel and channel belt dimensions.

238 These data are summarized in the channel belt aspect ratio (G), where submarine channel

239 belts are  $\sim 10\times$  lower aspect (i.e., thick and narrow) as compared to fluvial channel belts.

240

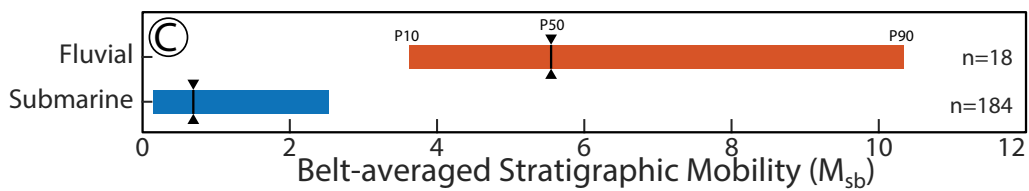
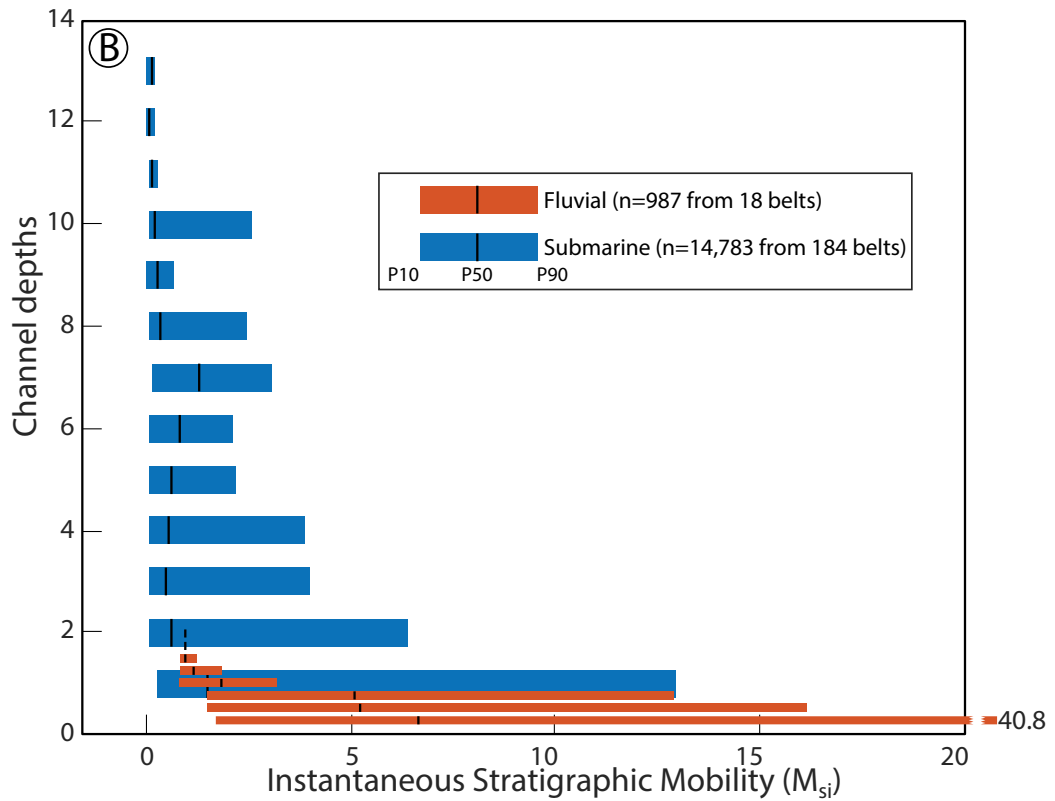
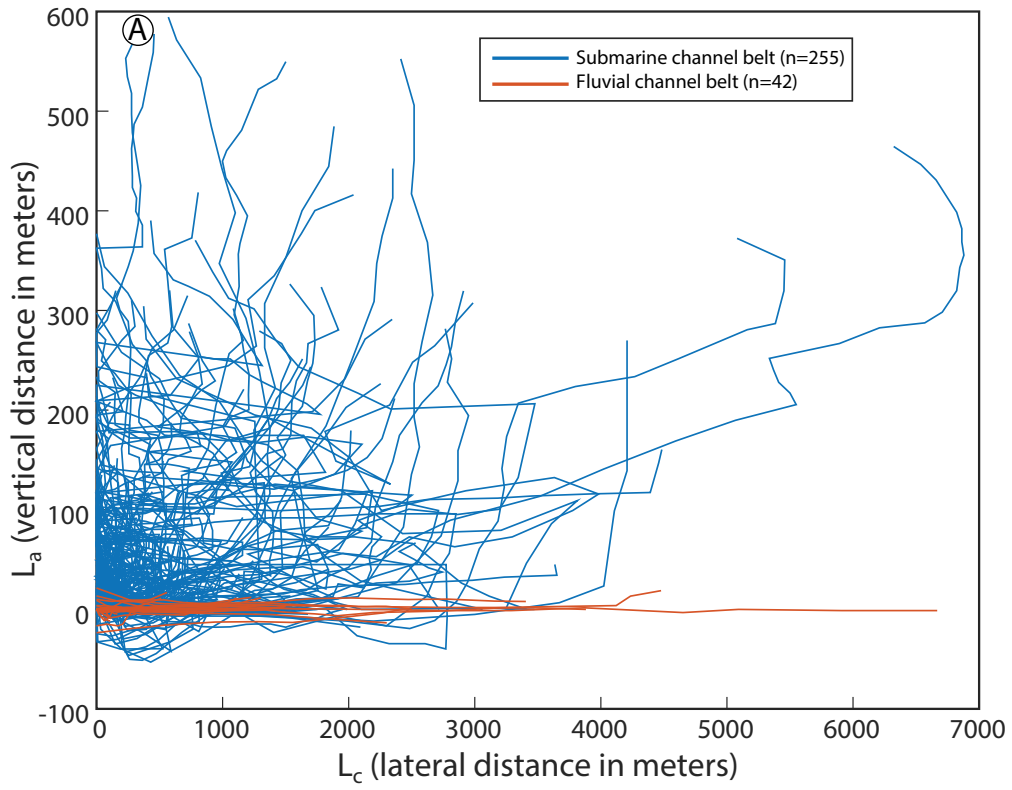


241

242 Figure 3. Stratigraphic trajectory and mobility measurements. A: Trajectories (i.e.,  
243 kinematic paths) of submarine and fluvial channel belts. B: Plot of Local stratigraphic  
244 mobility  $M_{sl}$  versus the height above the channel-belt base ( $z$ ) normalized by the channel  
245 thickness  $H$ . Submarine and fluvial channel belts have similar kinematic pathways, but  
246 submarine channels have  $\sim 10\times$  more aggradation. C: Distribution of belt-averaged  $M_s$   
247 ( $M_{sb}$ ), with submarine systems displaying  $10\times$  lower values (i.e., less lateral migration  
248 and more aggradation) than fluvial systems.

249

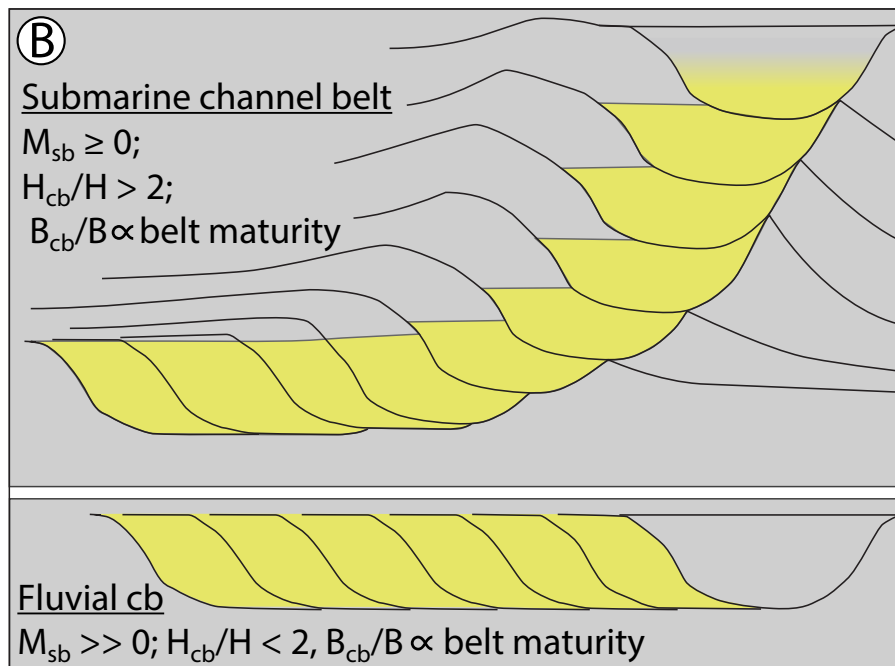
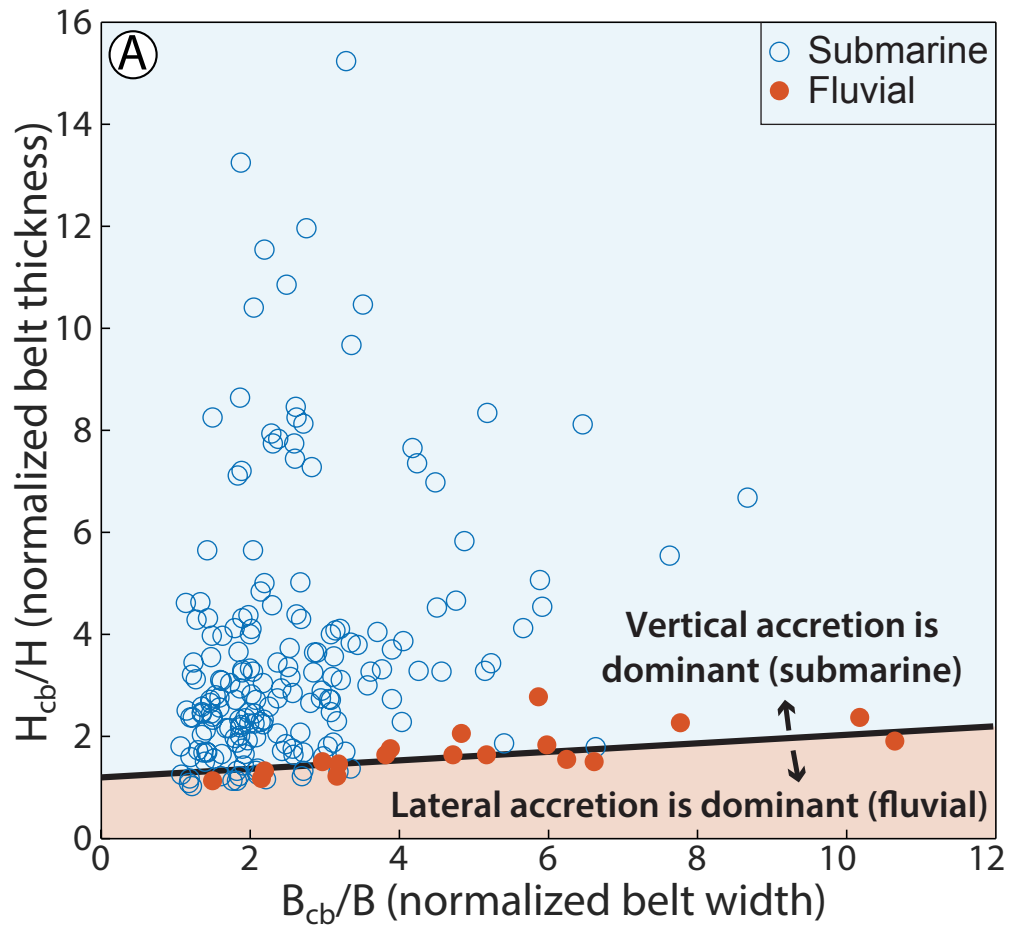




250

251 Figure 4. A: Normalized channel belt dimension cross-plot. Dashed line separates the  
252 dominance of lateral and vertical accretion deposits. Submarine channel belts are  
253 dominated by 'vertical accretion' rather than lateral accretion. B: Summary diagram of  
254 the stratigraphic architecture of submarine and fluvial channel belts.

255

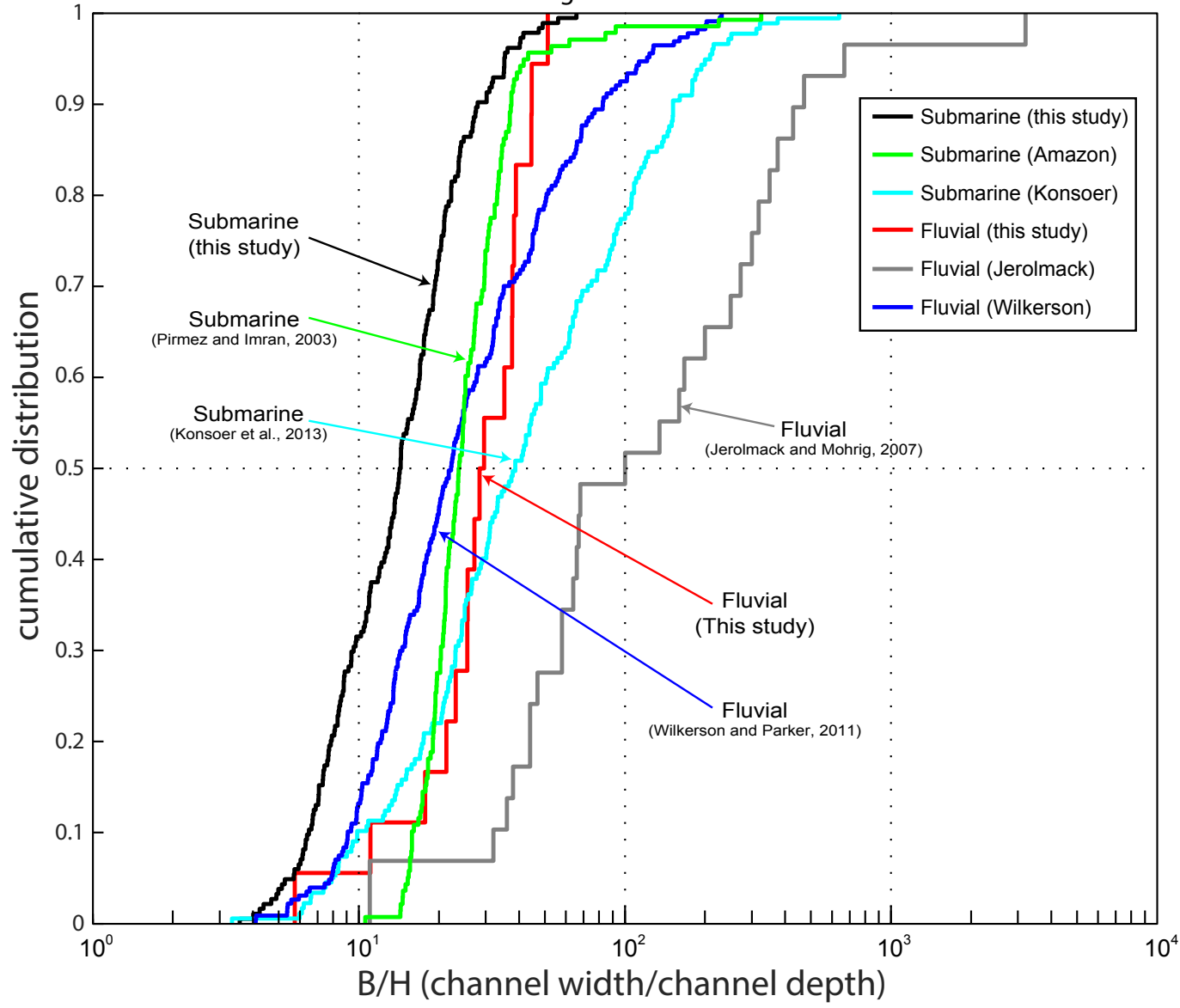


256

257 <sup>1</sup>GSA Data Repository item 2016xxx, data collection methodology and channel  
258 dimension data, is available online at <http://www.geosociety.org/pubs/ft2016.htm> or on  
259 request from [editing@geosociety.org](mailto:editing@geosociety.org).

260

Figure S1



261

262 **REFERENCES CITED**

- 263 Abreu, V., Sullivan, M., Pirmez, C., and Mohrig, D., 2003, Lateral accretion packages  
264 (LAPs): An important reservoir element in deep water sinuous channels: Marine and  
265 Petroleum Geology, v. 20, p. 631–648, doi:10.1016/j.marpetgeo.2003.08.003.
- 266 Allen, J.R.L., 1965, A Review of the Origin and Characteristics of Recent Alluvial  
267 Sediments: Sedimentology, v. 5, p. 89–191, doi:10.1111/j.1365-  
268 3091.1965.tb01561.x.
- 269 Deptuck, M.E., Sylvester, Z., Pirmez, C., and O’Byrne, C., 2007, Migration-aggradation  
270 history and 3-D seismic geomorphology of submarine channels in the Pleistocene  
271 Benin-major Canyon, western Niger Delta slope: Marine and Petroleum Geology,  
272 v. 24, p. 406–433, doi:10.1016/j.marpetgeo.2007.01.005.
- 273 Dorrell, R.M., Burns, A.D., and McCaffrey, W.D., 2015, The inherent instability of  
274 leveed seafloor channels: Geophysical Research Letters, v. 42, p. 4023–4031,  
275 doi:10.1002/2015GL063809.
- 276 Hodgson, D.M., Di Celma, C.N., Brunt, R.L., and Flint, S.S., 2011, Submarine slope  
277 degradation and aggradation and the stratigraphic evolution of channel-levee  
278 systems: Journal of the Geological Society, v. 168, p. 625–628, doi: 10.1144/0016-  
279 76492010-177.
- 280 Imran, J., Parker, G., and Pirmez, C., 1999, A nonlinear model of flow in meandering  
281 submarine and subaerial channels: Journal of Fluid Mechanics, v. 400, p. 295–331,  
282 doi:10.1017/S0022112099006515.

- 283 Jerolmack, D.J., and Mohrig, D., 2007, Conditions for branching in depositional rivers:  
284 Geology, v. 35, p. 463–466, doi:10.1130/G23308A.1.
- 285 Jobe, Z.R., Sylvester, Z., Parker, A.O., Howes, N., Slowey, N., and Pirmez, C., 2015,  
286 Rapid Adjustment of Submarine Channel Architecture to Changes in Sediment  
287 Supply: Journal of Sedimentary Research, v. 85, p. 729–753,  
288 doi:10.2110/jsr.2015.30.
- 289 Kneller, B., 2003, The influence of flow parameters on turbidite slope channel  
290 architecture: Marine and Petroleum Geology, v. 20, p. 901–910,  
291 doi:10.1016/j.marpetgeo.2003.03.001.
- 292 Kolla, V., Posamentier, H.W., and Wood, L.J., 2007, Deep-water and fluvial sinuous  
293 channels—Characteristics, similarities and dissimilarities, and modes of formation:  
294 Marine and Petroleum Geology, v. 24, p. 388–405,  
295 doi:10.1016/j.marpetgeo.2007.01.007.
- 296 Kolla, V., Bandyopadhyay, A., Gupta, P., Mukherjee, B., and Ramana, D.V., 2012,  
297 Morphology and internal structure of a recent upper Bengal fan-valley complex, *in*  
298 Prather, B.E., et al., eds., Application of the Principles of Seismic Geomorphology to  
299 Continental-Slope and Base-of-Slope Systems: Case Studies from Seafloor and  
300 Near-Seafloor Analogues: Society for Sedimentary Geology Special Publication 99,  
301 p. 347–369, doi:10.2110/pec.12.99.0347.
- 302 Macauley, R.V., and Hubbard, S.M., 2013, Slope channel sedimentary processes and  
303 stratigraphic stacking, Cretaceous Tres Pasos Formation slope system, Chilean  
304 Patagonia: Marine and Petroleum Geology, v. 41, p. 146–162,  
305 doi:10.1016/j.marpetgeo.2012.02.004.

- 306 McHargue, T., Pyrcz, M.J., Sullivan, M.D., Clark, J.D., Fildani, A., Romans, B.W.,  
307 Covault, J.A., Levy, M., Posamentier, H.W., and Drinkwater, N.J., 2011,  
308 Architecture of turbidite channel systems on the continental slope: Patterns and  
309 predictions: *Marine and Petroleum Geology*, v. 28, p. 728–743,  
310 doi:10.1016/j.marpetgeo.2010.07.008.
- 311 Mohrig, D., Heller, P.L., and Paola, C., 2000, Interpreting avulsion process from ancient  
312 alluvial sequences: Guadalupe-Matarranya system (northern Spain) and Wasatch  
313 Formation (western Colorado): *Geological Society of America Bulletin*, v. 112,  
314 p. 1787–1803, doi:10.1130/0016-7606(2000)112<1787:IAPFAA>2.0.CO;2.
- 315 Paola, C., and Voller, V.R., 2005, A generalized Exner equation for sediment mass  
316 balance: *Journal of Geophysical Research*, v. 110, F04014, 8 p.
- 317 Peakall, J., McCaffrey, B., and Kneller, B., 2000, A Process Model for the Evolution,  
318 Morphology, and Architecture of Sinuous Submarine Channels: *Journal of*  
319 *Sedimentary Research*, v. 70, p. 434–448, doi:10.1306/2DC4091C-0E47-11D7-  
320 8643000102C1865D.
- 321 Piper, D.J.W., and Normark, W.R., 1983, Turbidite depositional patterns and flow  
322 characteristics, Navy Submarine Fan, California Borderland: *Sedimentology*, v. 30,  
323 p. 681–694, doi:10.1111/j.1365-3091.1983.tb00702.x.
- 324 Sequeiros, O.E., Spinewine, B., Beaubouef, R.T., Sun, T., Garcia, M., and Parker, G.,  
325 2010, Characteristics of velocity and excess density profiles of saline underflows and  
326 turbidity currents flowing over a mobile bed: *Journal of Hydraulic Engineering*,  
327 v. 136, p. 412–433, doi:10.1061/(ASCE)HY.1943-7900.0000200.



- 328 Straub, K.M., Mohrig, D., McElroy, B., Buttles, J., and Pirmez, C., 2008, Interactions  
329 between turbidity currents and topography in aggrading sinuous submarine channels:  
330 A laboratory study: Geological Society of America Bulletin, v. 120, p. 368–385,  
331 doi:10.1130/B25983.1.
- 332 Sun, T., Meakin, P., Jøssang, T., and Schwarz, K., 1996, A Simulation Model for  
333 Meandering Rivers: Water Resources Research, v. 32, p. 2937–2954,  
334 doi:10.1029/96WR00998.
- 335 Sylvester, Z., Pirmez, C., and Cantelli, A., 2011, A model of submarine channel-levee  
336 evolution based on channel trajectories: Implications for stratigraphic architecture:  
337 Marine and Petroleum Geology, v. 28, p. 716–727,  
338 doi:10.1016/j.marpetgeo.2010.05.012.